Three-Dimensional Microscopy Using a Diffraction Grating Primary Objective

Thomas D. Ditto*
Aspex, Inc., 161 Hudson Street, New York, NY, 10013

ABSTRACT

Three-dimensional magnification of a diffusing surface can be achieved using profilometry based on holographic chirped frequency gratings and laser line projection. The recently patented method being investigated both supplants earlier 3-D microscopy methods using diffraction range finders and also competes favorably with extant confocal microscopy in coverage area, speed of acquisition and unit cost. The geometry of grazing incidence in a diffraction range finder shows an intrinsic anamorphic magnification. A narrow waist of input rays is expanded to the full width of the grating itself. The spatial magnification is simply the ratio of the length of the grating to the waist of the input column of rays. As the column of input rays approaches the grating plane, this magnification ratio approaches infinity. We develop a theory that predicts a limit to resolution as a function of illumination wave length and grating pitch of the primary objective. A simple microscope can achieve near micron resolution over several centimeters of depth in the visible light regime. An empirical demonstration is made using silver halide holograms.

1. INTRODUCTION

The discovery that higher-order diffraction images separate from the central zero-order as a function of the distance of a source of illumination to a diffraction grating was first disclosed in 1987.[1,2] The application of this principle to microscopy was demonstrated twelve years later with a diffraction grating primary objective.[3] In this demonstration, the grating did not magnify, but it did give range readings. Among the parameters used to define the grating, it was discovered that if the pitch of the grating grooves was varied according to a basic formula, the magnification power of the microscope could be achieved by the grating itself.

2. BACKGROUND AND THEORY

Near-field 3D profilometry can be achieved using variable pitch (chirped frequency) holographic optical elements (HOE's). The HOE is fabricated specifically in a manner that will reconstruct a wave front of an illuminated target inside a selected work volume, and a projected laser line sheet of light is used to interrogate the working volume for range and position of target surfaces that intersect the laser light. The method has been shown to overcome near-field blindness and perspective foreshortening endemic to almost all triangulation 3D profilometry systems. A prototype of a hand held scanner based on the method was developed under a 1995 Phase II NSF SBIR [4] and was named SBIR Sensor and Instrumentation of the Year prize by a NASA jury in 1997.[5] A disclosure on the prototype was published in *Optical Engineering* in 2000.[6] A patent for the method issued in the US in December 2002[7], and in 2003 the patent was allowed in Europe through the EPO.

Investigation of the diffraction range finding method has further revealed a magnification feature that can be achieved using the holographic chirped gratings in grazing incidence or grazing exodus configurations. The exodus configuration results in telescope instruments.[8 9 10] On the other hand, when the magnification is made at grazing incidence angles, the optics have leverage to resolve microscopic dimensions.

The geometry of grazing incidence in a diffraction range finder shows an intrinsic anamorphic magnification. A narrow waist of input rays is expanded to the full width of the grating itself. The spatial magnification is simply the ratio of the length of the grating to the waist of the input. See Figure 1.

* 3d@taconic.net ; http://home.earthlink.net/~scan3d

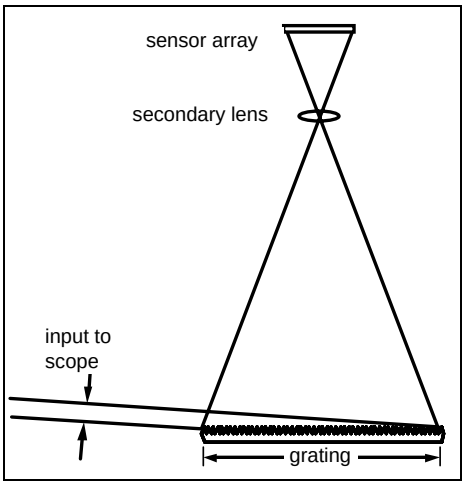

Fig 1 Anamorphic grating magnification

The author did not discover the anamorphic magnification feature of gratings. The phenomenon is a topic in teaching diffraction grating optics.[11] However, the utility of diffraction grating magnification in a range finder has not been studied, notwithstanding that the raw numbers suggest that the phenomenon has an application in 3D microscopy. As the input angle approaches grazing incidence, the ratio of the grating length to the input waist expands as the tangent of the angle of incidence, that is, with a limit at infinity.

Compared to refractive and reflective magnifiers, flat surface relief diffraction gratings lend themselves to grazing entry or exit configurations. Wavefront reconstruction at grazing angles proceeds as it does at any other angle. Efficiency losses are only introduced at angles of diffraction so close to evanescence that surface flatness restricts wavefront reconstruction. The tolerances for substrate flatness can be shown to be within typical float glass margins and easily within specifications of ½ wave optical flats.[12] Grazing incidence gratings have become part of the commercial lines of grating manufacturers and are routinely used for controlling laser wave length.

In order for periodic waves to be directed from a flat grating to a focal point grating, the specification for groove spacing must be variable pitch (a.k.a. chirped frequency). The grating can be manufactured holographically by duplicating the ray path desired on playback. The hologram is the intersection of a plane wave as referenced by a spherical wave. At any wave length of incident radiation λ, the pitch p of the resulting grating can be known from the angles of incident radiation i and reconstruction r.

(1) $$p = \frac{\lambda}{\sin(i) - \sin(r)}$$

In the case of a hologram where the incident angle i is a constant established by a plane wave and the angle of reconstruction r varies according to the angle determined by a spherical wave this relationship for pitch yields a hyperbolic variation in pitch length along the axis of the incident illumination.

We diagram the relevant parameters in Figure 2.

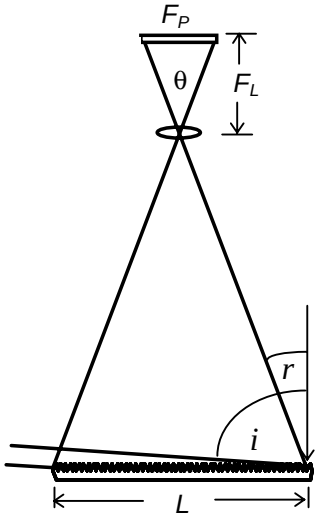

Figure 2 Parameterization of model

We are interested in grazing incidence angles, where $i \cong 89$ degrees. The reconstruction angles vary, but we know that the greatest magnification will occur on the axis of the grating normal, because it is along this axis that the secondary objective will have the widest field-of-view θ.

(2) $$\theta = 2\arctan\left(\frac{L}{2d}\right)$$

For a given focal plane width F_P there will be a focal length F_L for the secondary objective such that a grating of given length will fill the field-of-view.

(3) $$F_L = \frac{F_P}{2\sin\left(\frac{\theta}{2}\right)}$$

The grating period can be modeled for reconstruction by a specified secondary objective lens and a focal plane array of known length. We can say

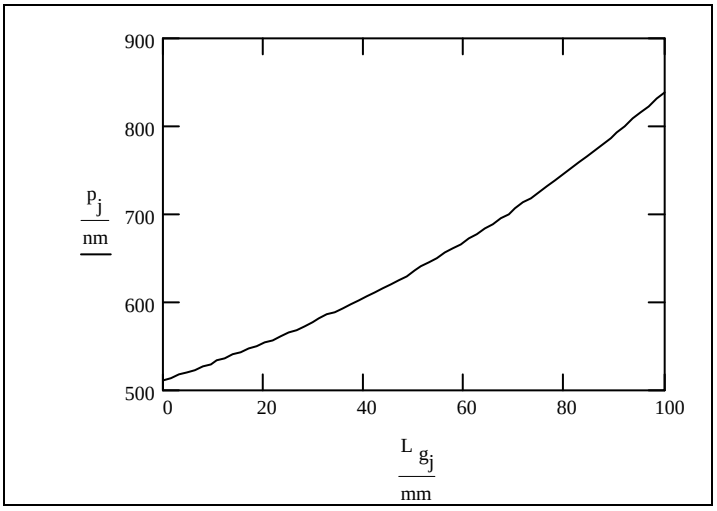

Figure 3 Grating pitch vs. grating length

$$r = \arctan\left(\frac{x}{F_L}\right) \quad (4)$$

where x is the displacement across the sensor array

As shown in Figure 3, this model produces non-linear hyperbolic frequency chirps in grating groove spacing as can be demonstrated in a sample calculation where

λ = 635 nm,
L = 100 mm,
d = 200 mm,
i = 88 degrees.

Diffraction range finding is a new optical technique that exploits the change in wavefront curvature as a function of the distance of a point source from a diffraction grating. In the extreme near-field there is a profound change in the incident angle of an off-axis wavefront striking the grating over very short range displacements. This change forces a shift in the position of an imaged diffraction order in a secondary receiver such as the lens and focal plane camera models in Figures 1 and 2.

3. PRACTICE

Diffraction range finding can be understood in the reduction-to-practice illustrated in Figure 5 which uses an interrogation beam in the form of a laser. For the sake of illustration, the grating illustrated is a transmission type. There is no significant difference in principle between reflection and transmission types with regard to the geometry. The laser is aimed into the region where diffraction will provide a signal on the focal plane of the secondary camera. When a target surface diffuses the radiation, the range to the target can be correlated with the displacement of the target as imaged in the camera.

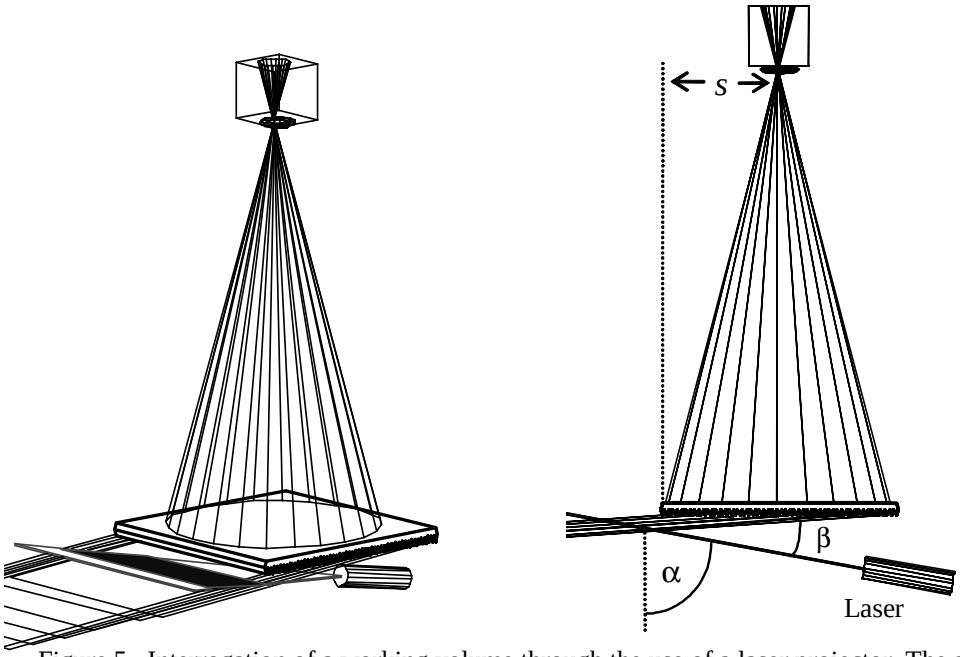

Figure 5 Interrogation of a working volume through the use of a laser projector. The angle of laser α affects the occlusion liability β. Stand-off s centers the camera relative to the grating length.

The range D as calculated along the length of the interrogation beam can be known from the angle r of reconstruction.

$$D = \frac{\kappa(d\tan(r) - s)}{\cos(\alpha) - \kappa\sin(\alpha)} \tag{5}$$

where

$$\kappa = \frac{\sqrt{1 - \left(n\frac{\lambda}{p} + \sin(r)\right)^2}}{n\frac{\lambda}{p} + \sin(r)} \tag{6}$$

and

$$s = \frac{L}{2} \tag{7}$$

Occlusion liability is determined by subtracting the laser angle from the incident angle

$$\beta = i - \alpha \tag{8}$$

The geometric optics model of a 3D microscope using a diffraction grating primary objective yields predictions of magnification and occlusion immunity that beg investigation because at angles of grazing incidence where the waist of the incident radiation is extremely narrow, the anamorphic magnification has leverage suggesting powers of 10. Moreover, when the grating is manufactured to a specification matched to intended angle of incidence, range acquisition falls along a linear displacement, in contrast with conventional triangulation designs which suffer from perspective foreshortening. Notably only the range dimension is magnified, so very large width to depth ratios are allowed.

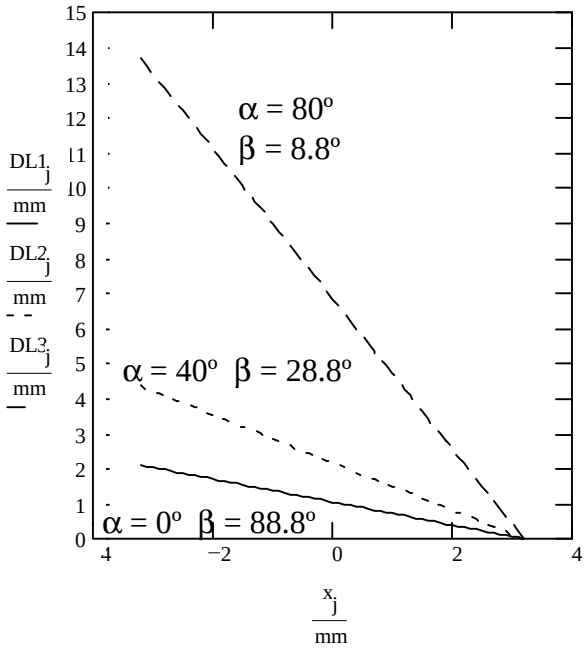

Figure 6 Range vs focal plane displacement for three angles of α and their correlated occlusion liabilities β

Consider the example case illustrated in Figure 3 where the angle of grazing incidence is 88 degrees, the secondary lens is 200 mm from a 100 x 100 mm grating. Using equations 5-8 we generate a graph of the range along the laser line DL vs. focal plane displacement x where the focal plane is 6.4 mm wide. We have selected three entry angles α for the interrogating laser: 0, 40 and 80 degrees. There is a tradeoff between depth and occlusion liability. However, even in the case where occlusion liability is less than 10 degrees, range bracket is 1.5 cm. Considering that the camera might well have 1500 photo sites, the nominal resolution would be 1 micron. In the other extreme where there is a high occlusion liability of 88.8 degrees, width to depth ratio is 50. The middle trace shows an occlusion liability of 28.8 degrees which is considered the conventional liability for most triangulation-based range finders. The ratio of width to depth is 20. This compares with cylindrical lens anamorphic magnifications which are typically no greater than 2:1.

The leverage afforded by the grazing angle is readily evident in telescopic applications where the grazing angle is in the exiting mode. We have used a precision linear chirp grating intended for use in the fabrication of Bragg gratings in optical fibers to obtain a the profile of a mannequin head with a grazing exodus angle of 80 degrees and an occlusion liability of 23 degrees, Figure 7(a).[7] The anamorphic magnification induced by the grating introduces a 5:1 improvement over conventional triangulation made at the same occlusion liability. Various angles of grazing exodus are illustrated in Figure 7(b) where the right hand image is the zero-order triangulation view, and the left hand profile is taken at the 80 degree grazing exodus angle.

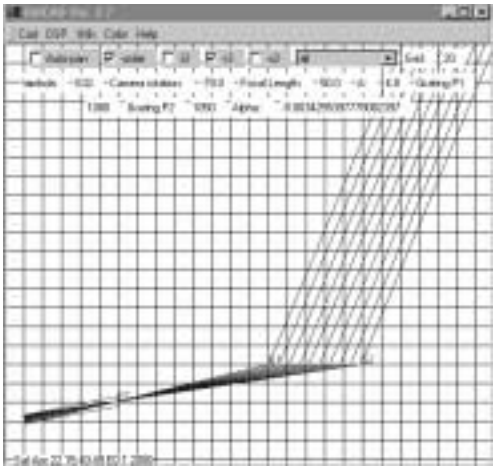

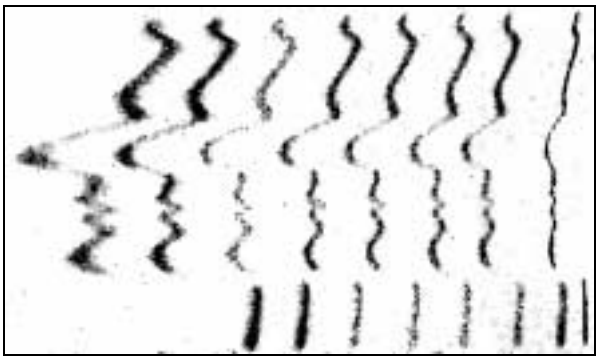

Figure 7 (left) The grating and camera for a telescope made using a linear chirp grating at 80 degrees grazing exodus Figure 7(right) A sequence of profiles taken of a bust.

Grazing exodus illustrated in Figure 7 is the converse of the proposed microscope that works in grazing incidence. Experiments with microscope optics have been carried out with a silver halide hologram made at incident angles of 70 degrees. Although well shy of the grazing angles possible with surface relief gratings, there is significant anamorphic magnification. In an experiment illustrated in Figure 8, a test block was illuminated by an interrogation beam 55 degrees off the grating normal.

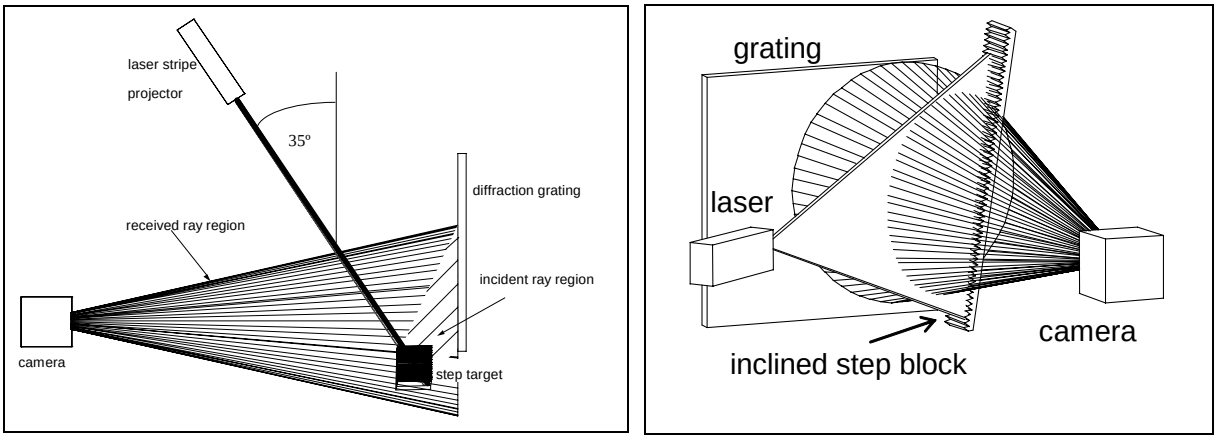

Figure 8 Bench setup with silver halide grating where target is a step block inclined at 10 degrees.

The image produced by the bench setup of Figure 8 is shown in Figure 9. Note that the direct view of the inclined step block is one fifth the displacement in the range dimension compared to the diffraction image, notwithstanding that the occlusion liability of the direct view is approximately the same as the diffraction image. This comparison is made by measuring the baseline of the inclined plane. The steps in the block are also magnified. Compare depth to height ratios between the diffraction and depth views as seen in the steps, and it is clear that the direct view is less than one, but the diffraction image shows a similar 5:1 ratio of depth to height. The step block itself consists of $1/10^{th}$ inch steps and is inclined at 10 degrees.

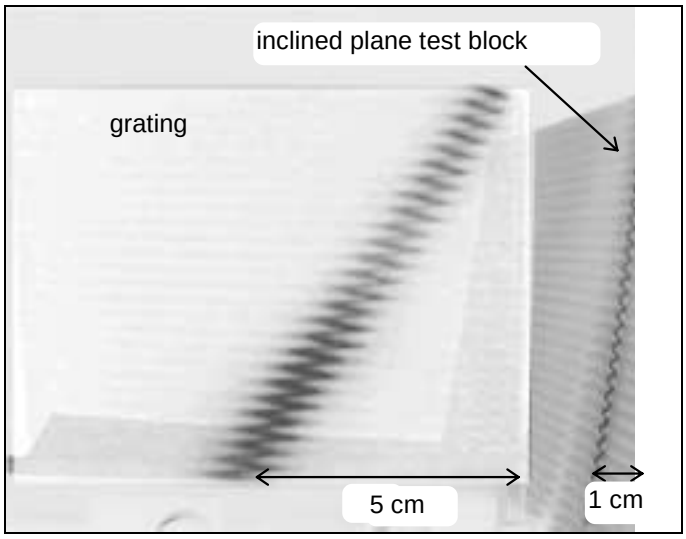

Figure 9 Focal plane image from Figure 8 bench setup

Another test with the silver halide grating compares the acquired profile where the occlusion liability can be known more precisely. A second camera was used to obtain a triangulation image at an occlusion liability angle of 20 degrees. The laser is at 10 degrees and the camera is rotated at 10 degrees. The grating was placed with care so that he incident angle upon the grating also was at 10 degrees. A diagram of the bench setup is shown in Figure 10. Note that the diffraction image camera also images the step target directly at an angle of approximately 70 degrees, so the setup is able to produce three different views from two cameras.

Triangulation images made at occlusion liability angles near 20 degrees with a lens wide enough to capture the same target length as the diffraction camera image or the triangulation image are so foreshortened as to provide little range data as can be seen from Figure 11 (a). Compare this to the diffraction image camera, Figure 11 (b) and (c). The diffraction camera triangulation image does have some useful data, but the diffraction image is has the benefit of anamorphic magnification and has the same occlusion liability as Figure 11 (a)..

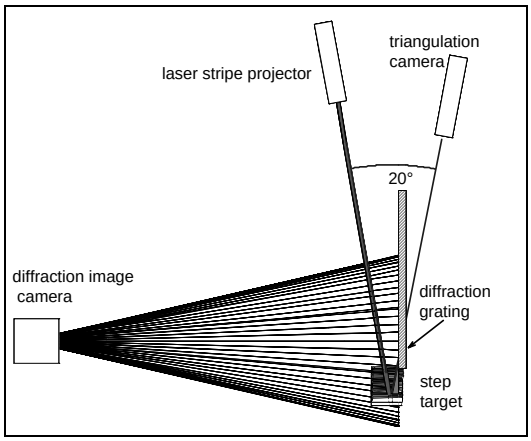

⇐ Figure 10
Comparative occlusion liability setup

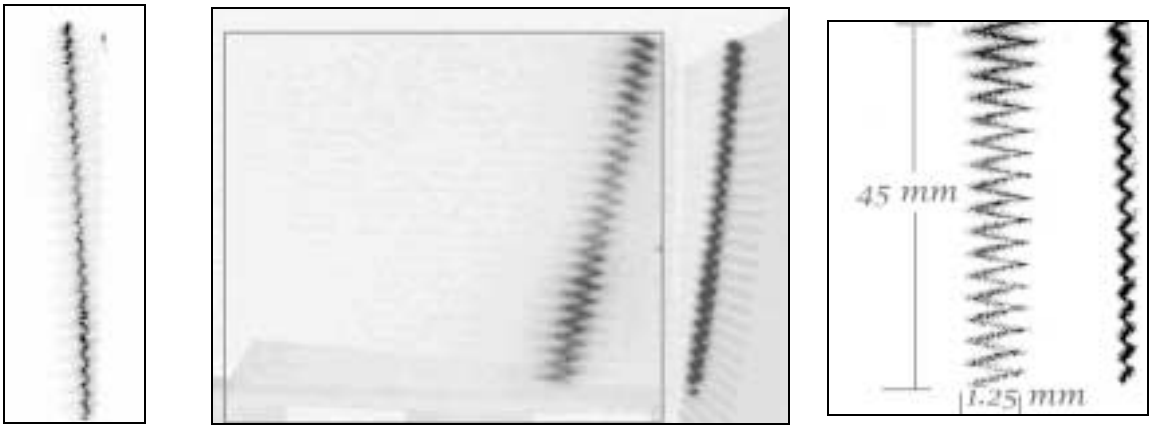

a b c

Figure 11 On the left (a) is a triangulation image with an occlusion liability of 20 degrees. The center image (b) is from the same setup but made with the diffraction grating camera. A comparison of the two images in (b) was made with incline removed and annotates the target's actual dimensions (c).

The silver halide hologram cannot be used at incident angles approaching 90º, because incident radiation would be reflected far more into the zero-order than diffracted into higher-orders. Methods have been developed to exploit index matching between the incident wave and the hologram that could be used,[13] although the superimposed substrates can introduce other artifacts. To date, these index matching methods are used as non-imaging optics where the grazing angle only provides background illumination flux.

It is a realistic objective to achieve grazing incidence for a microscope objective by using surface relief diffraction gratings, either in reflective or transmission modes. Gratings of this type can be modeled using iterative numerical solutions to Maxwell's equations, and a commercial software package PCGrate[14] predicts efficiencies of up to 40 per cent at angles of grazing incidence approaching evanescence.

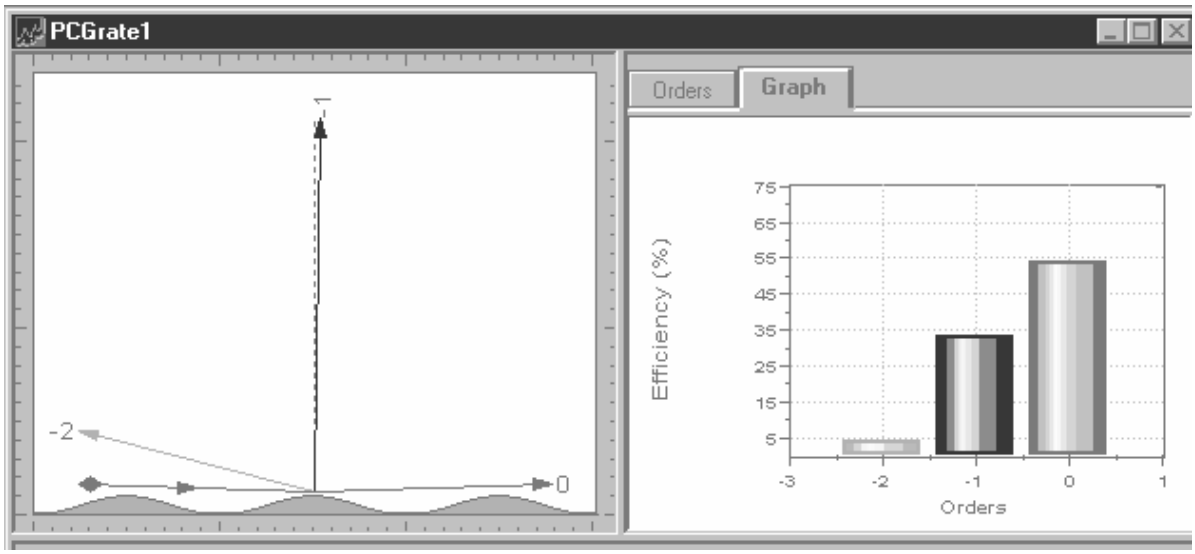

Figure 12 A prediction of PCGrate for 88º grazing incidence is a 35% efficiency in the first-order

The vendors of this software indicate that the predictions are unreliable at grazing angles, but the primary difficulty comes from predicting polarization rather than overall efficiency. It is well known experimentally that gratings with pitch lengths less than wave lengths of the incident radiation will have idiosyncratic swings in both efficiency and polarization. Typically these gratings are characterized by manufacturers empirically. On the other hand, the basic principles upon which interference of periodic wavefronts from a grating surface form higher diffraction orders is not changed, and surface relief gratings can be expected to produce useful efficiency, especially given the relative abundance of flux from projected lasers in the microscopic realm.

More problematic in realizing a practical microscope are the characteristics of laser illumination itself. Both the speckle artifacts and the relatively large footprint of a laser beam in the micron scale regime pose serious obstacles to exploiting the predicted magnification of grazing incidence diffraction grating optics.

In an earlier experiment [3] which used low frequency gratings as a grating objective in front of a conventional microscope objective, the author settled on an incoherent monochromatic light source created with incandescent illumination directed toward a dielectric bandpass filter that had a 5 nm cutoff. The instrument is illustrated in Figure 13(a). The bandpass filter eliminated speckle artifacts that had appeared when laser illumination was attempted. The speckle field is shown in Figure 13(b). However, high frequency diffraction grating optics are exquisitely sensitive to wavelength. Stable coherent laser illumination is preferable to incoherent radiation, even when filtered by a bandpass element. If laser speckle can somehow be restricted, the finesse of the depth resolution will be improved.

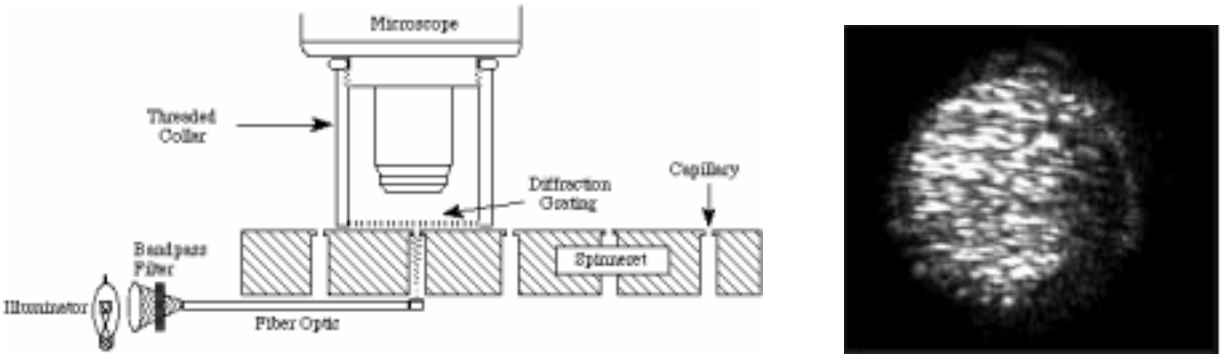

a b

Figure 13 Bandpass filter on an incandescent delivered by fiber (a) Laser speckle at micron scale (b).

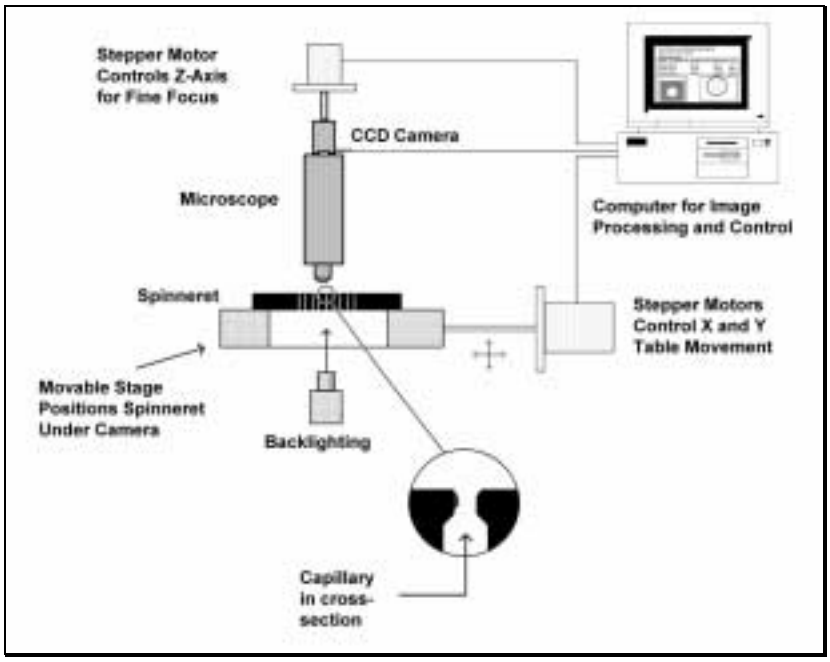

Figure 14 The Aspex SpinTrak®, a commercial optical inspection instrument

Speckle is an artifact of translational phase differences. It can be eliminated by active translation of a target surface over an exposure period long enough for energy to average itself to a constant level. The Aspex SpinTrak®, Figure 14, is an inspection instrument that uses a computer controlled motion platform to position objects that vary in surface area from centimeter to meter scale and have micron scale features. The computer controlled motion platform has repeatability and accuracy that can be measured in microns. The proposed diffraction grating microscope can be mounted on extant SpinTrak® platforms simply by switching out its present 2D microscope. Motion exposures can be used to evaluate speckle elimination by means of target translation.

A motion platform is required for the proposed microscope, because the 3D acquisition is in the form of a profile. Area scans do require a translation in one axis. The SpinTrak® platform or some other motion platform is a specification regardless of the utility of motion for speckle removal.

Laser projectors using diode optics are routinely focused to diameters of 30 microns for conventional triangulation 3D profilometry over working distances of several centimeters. This footprint is larger than the resolution afforded by the diffraction grating primary objective by an order of magnitude in the depth dimension. However, due to the anamorphic characteristic of diffraction grating magnification, the footprint problem is somewhat different in the length of the profile, since its profile length is not magnified by the grating. An area to investigate would be possible refinements to laser diode optics that might benefit this special condition, especially given the fact that laser diodes are intrinsically elliptical in their power distribution and must be corrected to form circular beams.

The grating needed for this project is a variant of the etched glass substrate types used in the marketplace of grating masters for the manufacture of Bragg gratings in optical fibers. These gratings are holographic chirped frequency gratings with zero-order suppression. The latter feature is not mandatory for this application, and Littman-Metcalf type grazing incidence gratings made for variable frequency lasers would work if these gratings had variable pitch.

4. RESOLVING POWER

Regardless of the quality and efficiency of the primary objective diffraction grating, the geometric optics prediction of infinite magnification is meaningless, since the wave nature of light restricts resolution to the phase interference between radiators on the incident wavefront itself. In refractive microscope optics this phenomenon is called the diffraction limit. The problem has been studied with diffraction gratings where it is referred to as the resolving power. Plane grating resolving power R is well understood when the object of study is separation of spectral lines.[15] In such studies, the resolving power is defined as the ratio of a wavelength to the smallest resolved portion of the wave length under study. $R = \lambda / \Delta\lambda$. The physical optics of resolving power can be reduced to the expression $R = | nN |$ where N is the absolute number of grooves in a plane grating and n is the diffraction order. Regardless of the diffraction order, the maximum achievable spectral resolution of a plane grating is dependent solely upon the considerable width W of the grating in the direction perpendicular to the grooves. It is said that $R_{MAX} = 2W / \lambda$. This is the diffraction limit.

Resolution of a diffraction range finder where the grating is plane grating with regular line spacing can be similarly analyzed. The distance resolving power R_d of a diffraction range finder can be predicted by correlating path lengths for the shortest discernable increments of change in distance.

(9) $$R_d = DL / \Delta DL$$

Changes in path length at the grating are a caused by changes in range positions of a target as detected at some fixed wave length λ. The smallest resolvable shift between positions is caused by the phase shift of the measured wave length as the target changes in range. Unlike spectral resolution where changes in wave length cause shifts in the angle of diffraction and where the width of the grating is directly proportional to the resolving power, range resolution is determined by the parameter p, the pitch of the grating. As pitch increases, resolution decreases, that is, R_d is inversely proportional to p.

Consider the geometry in Figure 15.

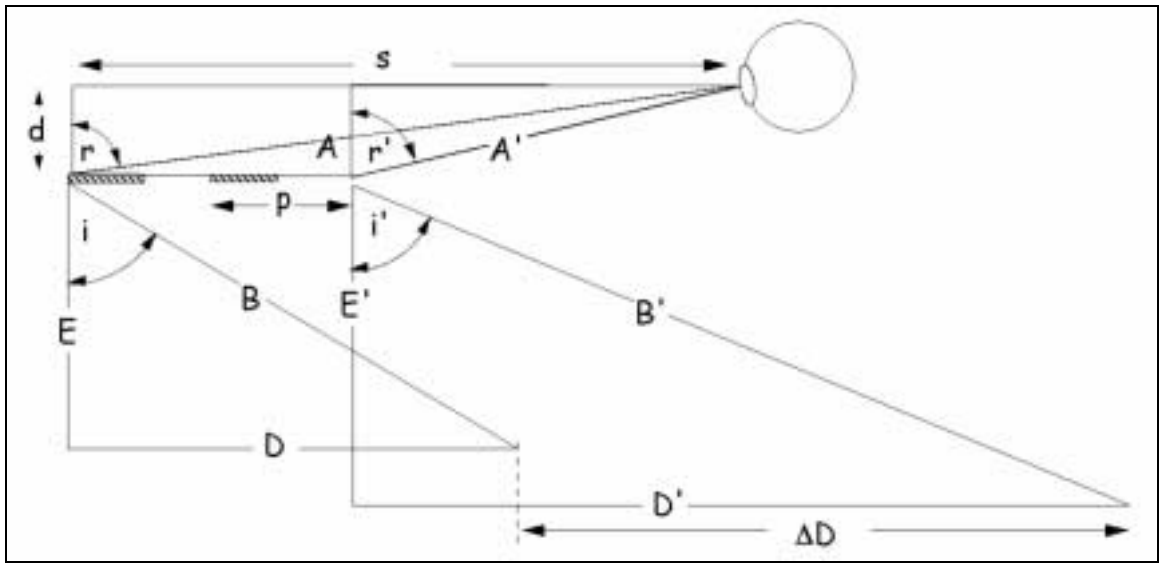

Figure 15 A generalized model for diffraction range finder resolution calculation

Two adjacent grating grooves of length p are shown. To observe a transition of the target from distances D to D', a phase change must exist between the ray paths AB and $A'B'$ sufficient to cause a perceptible extinction of a wave length λ. A complete extinction occurs at the half wave length, so for a resolvable increment of range ΔD it can be argued that

$$A + B = A' + B' - \frac{\lambda}{2} \tag{10}$$

ΔD itself is the difference between D' and D at the offset of $2p$. In other words:

$$\Delta D = 2p + D' - D \tag{11}$$

To match the grating for the distances being ranged, legs D and E (Figure 15) can be entered into the Diffraction Equation along with parameters s and d for the location of the sensor to specify the pitch p. (Note that the order $n = 1$ is being used, so this term is not needed and will be dropped from subsequent expressions).

$$r = \arctan\left(\frac{s}{d}\right) \tag{12}$$

$$p = \frac{\lambda}{\sin(i) + \sin(r)} \tag{13}$$

According to the geometry of Figure 15 these identities also apply:

$$A = \frac{d}{\cos(r)} \tag{14a}$$

$$B = \frac{D}{\sin(i)} \tag{14b}$$

The triangle $A'D'E'$ must be calculated. To do this we determine angle i' which is dependent upon r' by virtue of the Diffraction Equation where $\sin(r') + \sin(i') = \lambda / p$.

First:

$$r' = \arctan\left(\frac{s - 2p}{d}\right) \tag{15}$$

Then:

$$i' = \arcsin\left(\frac{\lambda}{p \sin(r')}\right) \tag{16}$$

As per Equation (10) we can say:

$$B' = A - A' + B + \frac{\lambda}{2} \tag{17}$$

where

$$A' = \frac{d}{\cos(r')} \tag{18}$$

$$D' = B' \sin(i') \tag{19}$$

The procedure for calculating the resolution limit of a diffraction grating primary objective calibrates the potential for 3D range acquisition better than the simple geometric optics of grazing incidence derived in equations (1-8). Those equations can produce erroneous predictions. For example, if the grazing angle is set to 89.9 degrees the magnification is 1000 times. (Figure 16). This is an exaggerated figure that simply is not possible in the real world due to the wavelength of light.

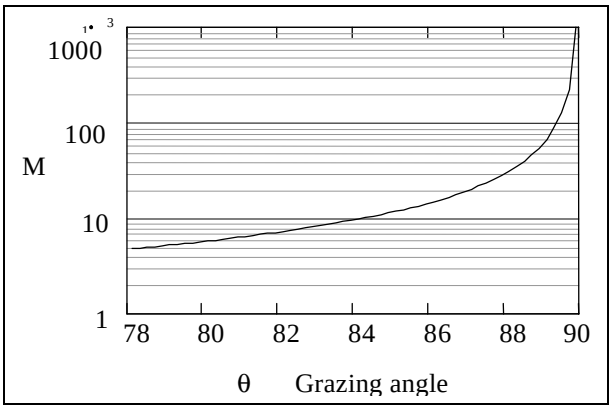

Figure 16 Magnification without concern for diffraction limit. Log scale

A sample calculation using the definition of ΔD from equations (9-17) shows that the shortest distance that can be resolved decreases to a limit as the angle of incidence approaches 90 degrees. Given a baseline of 10 cm from target to grating (as would apply in a microscope of the type diagrammed in Figure 5) and where the wave length is 635 nm, the resolution at the center of the grating could vary from 3.5 to 2.2225 microns as the incidence angle varied from 45 degrees to 90 degrees (see Figure 17).

Compared to a conventional microscope, a diffraction limit of 2.6 microns at 635 nm is more than the comparable limit for refraction objectives in 2D, but such objectives must be refocused for each 3D plane, and moreover, the diffraction limit also goes up as the specimen increases in distance. This is why conventional microscope objectives have a planar face on the specimen side and why the best resolution is achieved with oil immersion.

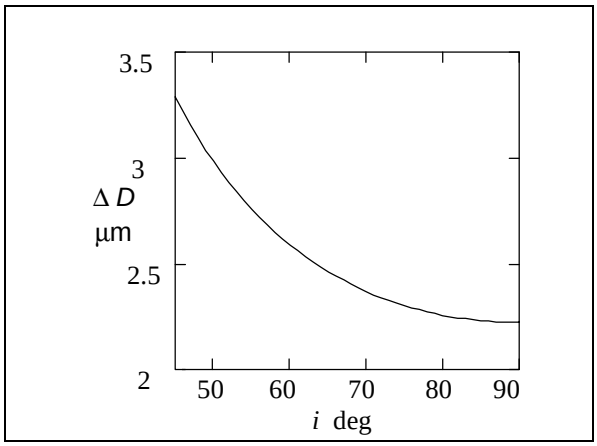

Figure 17 A prediction using a resolving power model Resolution vs. angle of incidence for targets at 10 cm from the grating center.

There are many other ways of using the same set of equations for evaluation and optimization. For example, it can be shown that with a grating stand-off to target of 1 cm, the theoretical range resolution decreases to 1.65 microns for light of wave length 635 nm. It is self-evident that the resolution can be improved by the use of shorter wave lengths, as is now possible with the new generation of blue and ultra violet laser diodes. Interestingly, the resolution remains quite good at very great distances from the grating. For example, the model predicts 6 mm resolution at 1 km. As a range finder, the grazing incidence configuration might serve at kilometer scale provided the target has sufficient flux to be detected. As with all new technologies, we are encountering some unexpected predictions that suggest novel applications.

In order to fully examine the potential of grazing incidence diffraction range finders in either their microscopic or telescopic regimes, it would be prudent to refine the resolution model. Scalar and vector diffraction theory can be studied.

Of course, the data must be acquired and processed. The diffraction limit is not the statistical limit of the resolution, since the receiving camera will have multiple photosites illuminated by the higher-order flux. The spatial energy on these sites is distributed in a Gaussian bell curve that can be converted into an subpixel position estimate. In most cases, such estimates increase the effective resolution of the range finder by a factor of 4. As a practical matter, one could expect sub micron resolution in 635 nm illumination when the diffraction limit itself is greater than a micron. This statistical refinement takes advantage of multiple pixels and their gray scale content. As a rule, if the gray scale is eight bits, the resolution of a diffraction range finder can be increased by four bits over its nominal optical diffraction limit by taking the center of gravity.[16]

5. COMMERCIAL POTENTIAL

While it is always possible to make a two-dimensional image from a three-dimensional database, it is not usually possible to go the other way. Hence, an affordable 3D microscope could become the default for all users of microscopes if prices were competitive with conventional light microscopes.

Sales of all microscopes in year 2000 have been reported as $800 million in a marketplace that is dominated by visible light types.[17] Of this market, a microscope that would directly compete with a diffraction range finder type is the confocal type which was reported to have had a worldwide market in 2000 of $55 million or six per cent of the total market. Its market share continues to grow, and by 2001 confocal sales were reported to be 7.5% of the total world market.[18]

The argument for the commercialization of the diffraction grating primary objective microscope is that compared to the confocal design, the diffraction primary 3D microscope acquires data faster yet is less

expensive to manufacture. Confocal microscopes cost six figures and can take minutes of operation to assemble a scan over several centimeters. The price point for the first commercial diffraction range finder microscopes is expected to be one half to one tenth that of the confocal alternative and the rate of acquisition would be from 10 to 1000 times faster depending upon profile length.

Aspex is a small company that enjoys deep penetration into a niche microscope market. It can immediately exploit the 3D microscopy technology in this niche where about 20% of its customers have already requested the 3D capabilities that come from the proposed instrument.

Specimen analysis in medicine, biology, geology, archeology and paleontology routinely involves microscopy. The addition of the 3rd dimension to any data base drawn for a volumetric specimen is clearly of great value. We do not have market data for these diverse scientific disciplines, but instrumentation is always a key capital outlay for these sciences, and companies like Nikon, Olympus, Zeiss, and Leica depend greatly on the scientific marketplace and its related component in education.

The author has personal experience in the dental applications of 3-dimensional microscopy from the brief period when the basic patent was licensed to Dimension Data, Inc. At that time he designed a hand held 3D camera meant for *in vivo* digitization of teeth. The author may both draw from that experience which could lead to an embodiment for diagnostic applications in dentistry. It is also anticipated that related embodiments drawn from knowledge gained in studying the grazing incidence configuration will lead to endoscopes for use in medicine.

Footnotes

[1] Thomas DeWitt, *Range Finding by Diffraction*, U.S. Patent 4,678,324, July 7, 1987

[2] Tom DeWitt, "Novel methods for the acquisition and display of three-dimensional surfaces," *Optical and Digital Pattern Recognition*, 1987, SPIE, Vol. 754, pp. 55-63

[3] Thomas D. DeWitt and Douglas A. Lyon, "Three-dimensional microscope using diffraction gratings," *Three-Dimensional and Unconventional Imaging for Industrial Inspection and Metrology*, SPIE, Vol. 2599, pp. 228-239

[4] DMI-9420321 “A Hand-Held Three Dimensional Scanner”

[5] *NASA Tech Briefs*, Technology 2007, “Small Business Stars”, December 1997, Vol. 21 No. 12, p. 32

[6] Tom Ditto and Douglas A. Lyon, "Moly a prototype handheld three-dimensional digitizer with diffraction optics," *Optical Engineering*, January 2000, Vol 39 No. 1, pp. 68-78

[7] Thomas D. Ditto and Douglas A. Lyon, “Variable grating for diffraction range finder”, US Patent 6,490,028, Dec. 3, 2002

[8] Tom Ditto and Douglas A. Lyon, "Anamorphic magnification using a chirped grating in grazing incidence mode" *Conference on Machine Vision and Three-Dimensional Imaging Systems for Inspection and Metrology*, October 2000, SPIE Vol 4189 paper 19

[9] Tom Ditto, "Compact 3D Profilometer with Grazing Incidence Diffraction Optics," *Proceedings of the Third International Conference on 3-D Digital Imaging and Modeling*, IEEE Computer Society, PR00984, June 2001 pp. 73-80

[10] Tom Ditto, “The Dittoscope,” *Future Giant Telescopes*, SPIE Vol. 4840, August, 2002

[11] Christopher Palmer, *Diffraction Grating Handbook*, 2nd Edition, Milton Roy Company, 1994, p.9

[12] Tom Ditto, “An approximation of the effect that uneven grating causes in the distribution of the spectrum,” http://www.drillamerica.com/PDF/plate_calc.pdf

[13] Nicholas J. Phillips et al, “Grazing incidence holograms and system and method for producing the same,” U.S. Patent No. 5,822,089, October 13, 1998

[14] http://www.pcgrate.com

[15] Christopher Palmer, *Op. Cit.*, p.7

[16] H.C van Assem, M. Egmont-Petersen, J.H.C. Reiber, “Accurate object localization in gray level images using the center of gravity measure; accuracy versus precision,” *IEEE Transactions on Image Processing*, volume me 11 (2002)

[17] Market Forecasts “Microscopy Markets” http://www.bizintelagents.com/reports/tk12574_microscopy.html

[18] http://www.the-infoshop.com/pdf/tk12574.pdf p. 5